# A computer-aided Detection of Cerebral Microbleeds on Minimum Intensity Projection MR images of SWI

Wei Bian[1,2], Christopher P Hess[2], Susan M Chang[3], Sarah J Nelson[1,2], and Janine M Lupo[2]

*[1]Graduate Program in Bioengineering, University of California San Francisco & Berkeley, San Francisco, CA, United States, [2]Radiology and Biomedical Imaging, University of California San Francisco, San Francisco, CA, United States, [3]Neurological Surgery, University of California San Francisco, San Francisco, CA, United States*

**Introduction**: The recent interest in exploring clinical relevance of cerebral microbleeds (CMBs) in cerebral amyloid angiopathy[1], neurodegenerative diseases[2], and radiation injury in brain tumors[3] has motivated the need for a fast and accurate method for their detection. However, their small size and wide distribution render the visual inspection of CMBs on MR images a lengthy task that is highly prone to human error. While several semi-automated CMB detection algorithms have been recently published[4-7], their detection sensitivity and computation time are still in need of improvement. In this study, we propose a new CMB detection method with higher sensitivity and faster computation. The method utilizes the 2D fast radial symmetry transform (FRST) to initially detect nearly all possible putative CMBs. Falsely identified CMBs are subsequently eliminated by examining geometric features measured after performing 3D region growing on the potential CMB candidates. The method is designed to identify CMBs on minimum intensity projected susceptibility-weighted MR images (mIP SWI) that have increased sensitivity to CMBs over magnitude images or unprocessed SWI images.

**Materials and methods**: Fifteen patients with CMBs induced by radiation treatment for resected gliomas were retrospectively selected to evaluate the performance of the proposed method. T2*-weighted MR images of the patients were acquired on a GE 3T scanner (GE Healthcare, Waukesha, WI) using a 3D spoiled gradient echo sequence with TE/TR=28/56ms, FA=20°, a resolution of 0.5x0.5 x2mm and 40 slices. Standard SWI post-processing techniques[8-9] were applied, and the skull and background were removed from reconstructed images by utilizing FSL's brain extraction tool. Images were then normalized to an intensity range of 0~255 and minimum intensity projected through 4 slices (8mm) with an overlap of 3 slices. CMBs were counted independently by two raters (CPH and JML), and discrepancies were resolved by consensus review. To construct a ground truth that comprises CMBs identified not only by visual inspection but also by automated detection, the raters initially counted CMBs using the proposed algorithm with parameters set for high sensitivity but low specificity, then distinguished true CMBs from false-positive CMBs and additionally searched for true CMBs missed by the algorithm.

An overall scheme of our detection algorithm is shown in Fig.1. The first step in our detection algorithm was to use the gradient-based transform FRST to highlight circular features on images. The parameters of the FRST were empirically selected such that in this initial step the transform would identify the greatest possible number of true CMBs, regardless of the number of false positives. Pixels that had an absolute transform value |S| above 170 were directly identified as CMB candidates, while pixels with smaller |S| needed to undergo subsequence steps that maximized the sensitivity to low contrast CMBs while greatly reducing the number of false positives. False positive reduction begins with screening the FRST output with a vessel mask, which is also generated using the FRST by computing the orientation projection map *O* at radius of 1. The map is then used to create a binary mask in which a pixel value is 1 if its value on *O* decreased by at least one unit from its initial value. The mask highlights vessels and the edges of brain, regions where CMB mimics are typically found. In the next step, 3D locally connected regions are created from the pixels that passed the vessel mask screening, and 3D region growing is performed thereafter to grow each local region to its full extent in order to quantify 2D geometrical features of area, circularity and centroid. These features are preferred over 3D features such as volume and sphericity, which are distorted after mIP processing. Threshholds of these features were empirically chosen based on prior information of targeted CMBs, and were used to construct classifiers to distinguish true CMBs from false positives. The outputs from the classifiers were considered CMB candidates and subjected to visual inspection.

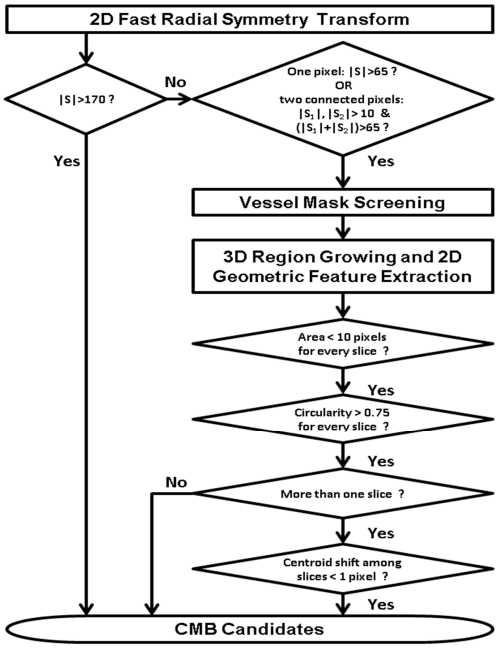


**Figure 1.** Schematic diagram for the proposed CMB detection algorithm and selected optimized parameters.

**Results**: A total of 420 true CMBs (mean diameter: 1.25mm or 2.05 pixels) were identified from 15 patients, of which 371 were correctly detected by our algorithm, resulting in a sensitivity of 88.3%. The initial detection using the FRST identified 4750 potential CMB candidates, 92% of which were false positives. If the vessel mask had not been used, the number of false positives would have been 6 times as large. After region growing, 83.7% of these false positives were eliminated with a final average of 47.4 false CMBs identified per patient (range 23~64). The computation time of the algorithm was only 1 minute per patient using one core of a Linux workstation with 8 GB of RAM.

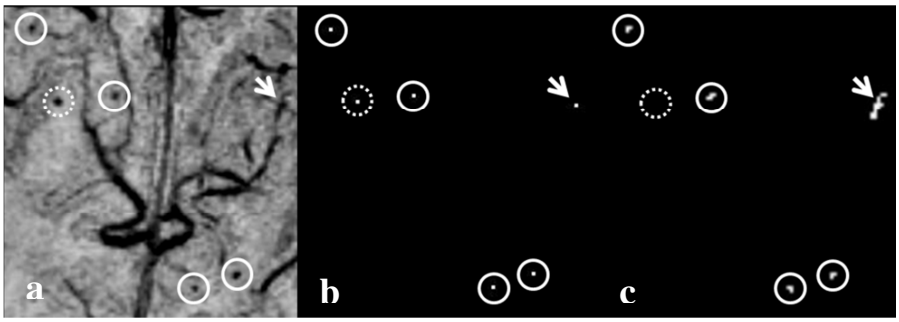


**Figure 2.** Representative examples of CMBs detected by our algorithm. The center of 5 CMBs (circles) and 1 false positive (arrow) from a vessel on mIP SWI image (a) are highlighted on the FRST map (b). After 3D region growing and geometric feature examination, all true CMBs were identified and the false positive was eliminated because of the linear shape of its grown region (c). One true CMB (dashed circle) was directly identified because its |S|>170, and did not undergo subsequent analysis.

**Discussion and Conclusions**: Achieving high sensitivity was the top priority in designing our algorithm, because visual inspection to remove false positives is far easier than identifying CMBs missed by the detection algorithm. Our algorithm achieved the highest sensitivity (88.3%) when compared to previous methods[4-7], with the next best[5] having a sensitivity of 81.7%. Moreover, our elevated sensitivity was achieved without compromising computation speed, with a processing time of 1 minute compared to times of 1 hour reported by others[5-6]. In terms of specificity, our algorithm produced more false positives (47.4 vs. 18.7 per patient) than the one proposed by Kuijf et al[6]. However, the latter used gray/white matter mask to remove confounding brain structures, which requires additional time for image registration and segmentation. Our CMBs also spanned a smaller number of pixels (average diameter: 2.05 vs. 2.28 pixels) than in Kuijf et al, which posed a greater challenge. As a result, we modified the FRST transform to specifically detect smaller, lower contrast radiation-induced CMBs and used it to generate a vessel mask that greatly reduced the number of false positives in the initial detection. Although the method was evaluated for CMBs arising in the setting of prior radiation therapy for gliomas, its performance should also make it an excellent method for detection of CMBs associated with other neurologic disorders

**References**: **1.** Greenburg SM et al., *Neurology* 1999;53:1135-1138. **2.** Cordonnier C et al., *Brain* 2011;134:335-344. **3.** Lupo JM et al., *Int J Radiat Oncol Biol Phys* 2012;82: 493-500. **4.** Seghier ML et al., *PLoS One* 2011;6:17547. **5.** Barnes SR et al., *Magn Reson Imaging* 2011;29:844-852. **6.** Kuijf et al., *Neuroimage* 2012;59:2266-2273. **7.** Kuijf et al., *ISMRM Proc* 2012;3762. **8.** Haacke EM et al., *Magn Reson Med* 2004;52:612-618. **9.** Lupo JM et al., *Magn Reson Imaging* 2009:27:480-488

*Acknowledgement*: This work was supported by UC Discovery grant ITL-BIO04-10148 and a fellowship from GEMS graduate training program.